JACS
JOURNAL OF THE AMERICAN CHEMICAL SOCIETY
Communication
pubs.acs.org/JACS

Biomimetic Superhelical Conducting Microfibers with Homochirality for Enantioselective Sensing

Wenjun Zou,[†,‡,§] Yong Yan,[†,§] Jin Fang,[†] Yang Yang,[†] Jie Liang,[†] Ke Deng,*[,†] Jianlin Yao,*[,‡] and Zhixiang Wei*[,†]

[†]National Center for Nanoscience and Technology, Beijing 100190, China
[‡]College of Chemistry, Chemical Engineering and Materials Science, Soochow University, Suzhou 215000, China

Supporting Information

ABSTRACT: Chiral amplification and discrimination are great challenges in both scientific and technological research fields such as chemical synthesis, chiral catalysis, and biomedicine. By mimicking protein superstructures in nature, chiral conducting polyaniline (PANI) molecules induced by chiral dopants were self-assembled to ultra-ordered superhelical microfibers. The induced homochirality is observed to be amplified into different hierarchies, from chiral molecules to helical nanostructures, and to superhelical microstructures. Furthermore, both experimental and theoretical results indicated that the gas sensor made from a single PANI helical microfiber showed enantioselective discrimination to chiral aminohexane, giving it great potential for applications in online chiral discrimination.

Chirality is one of the most important features of biomolecules; examples are the double helix of DNA and α-helix of proteins, owing to the homochirality of their components (D-sugars and L-amino acids). Controlled by non-covalent interactions, chirality of small molecules could be expressed at higher levels, from helical conformation of macromolecules to helical nanostructures and supramolecular structures, and even to superhelixes.[1−3] Inspired by the chiral biological structures in nature, a variety of functional structures with homochirality have been designed with unique electrical, optical, or magnetic properties.[4−7] Among those, conducting polymers comprise one type of multifunctional synthetic materials with excellent electrical, optical, and even biological activities.[8−10] Conducting polymers with homochiral conformation or supramolecular structures have been successfully induced by covalent or non-covalent bonded chiral groups,[11−14] but preparing higher order hierachical structures with homochirality remains a scientific challenge.

Among the multifunctional properties of chiral materials, enantioselective sensing is the most promising aspect because of the need for fast recognization of chiral drugs and even pheromones, like some insects. The existing techniques of chromatography and electrochemistry have been extensively studied in the detection and separation of enantiomers. However, the methods mentioned above are mostly carried out in an off-line way in solution.[15−21] Solid-state devices for chiral sensing *in situ* are highly desirable for both the material synthesis and device fabrication techniques.[22]

In this Communication, a typical conducting polymer, conducting polyaniline (PANI) helical microfibers composed of twisted helical nanofibers, is reported by mimicking protein superstructures. The hierachical chirality of microfibers was induced by chiral camphorsulfonic acid (CSA) as dopant and amplified by a subsequent self-assembly process. The ultra-ordered molecular arrangement and well-defined shapes of microfibers facilitate the fabrication of a single fiber, and prototype devices show enantioselective discrimination to chiral aminohexane.

In order to synthesize PANI helical microfibers, a PANI solution was first synthesized in the presence of CSA in a polymerization process (see experimental details in Supporting Information). A poor solvent herein, methanol was introduced to the solution of chiral PANI molecules, which were induced by chiral CSA in its good solvent (mixture of THF/$CHCl_3$ with a volume ratio of 1/3). Once the good-to-poor solvent ratio, denoted as [G]/[P], reached to 35%:65%, super-long (over 20 μm), single-handed helical microfibers were obtained by a slow self-assembly process, as show in Figure 1a−d. A high ratio of poor solvent resulted in quick precipitation of PANI, which is not favorable for forming ordered nanostructures or microstructures. Chiral CSA molecules played key roles in this system: First, CSA acted as a dopant to increase the solubility of PANI in the polymerization process, which is important to obtain a stable solution in its good solvent. Second, the steric hindrance of chiral CSA was the driving force for the formation of single-handed PANI and its helical fibers. The PANI helical microfibers showed enantiopure left-handed helical morphologies when S-CSA was used as dopant (Figure 1a and magnified SEM image in Figure 1b). However, right-handed helical microfibers were obtained when R-CSA was used as dopant, as shown in Figure 1c,d, which indicates that the chirality of helical microfibers is induced by chiral dopant acid.

Superhelical microfibers show much stronger absorption than chiral PANI molecules themselves in circular dichroism (CD) spectra (see Figure S1 in Supporting Information, and their morphology is given in Figure S2), indicating the amplification effects of CD signals due to $\pi-\pi$ stacking of chiral PANI molecules. Taking the S-CSA-doped PANI microfibers as an example, helical microfibers show a strong positive band at ~460 nm (Figure 1e), which is ascribed to the

Received: September 21, 2013
Published: December 26, 2013

dx.doi.org/10.1021/ja409796b | J. Am. Chem. Soc. 2014, 136, 578−581

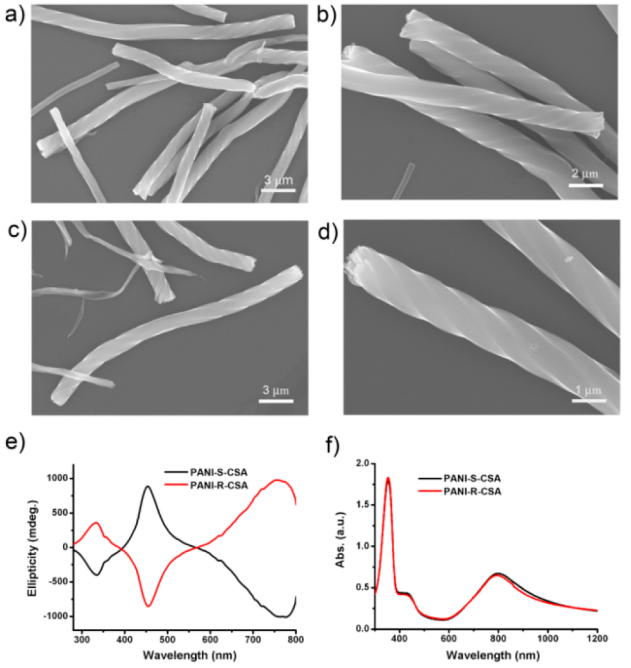

Figure 1. SEM images of PANI helical microfibers. (a,b) PANI helical microfibers induced by S-CSA as dopant, and very clear left-handed helical screws were observed. (c,d) Images of right-handed helical microfibers induced by R-CSA as dopant. (e) S-CSA- and R-CSA-doped PANIs showed mirror images in CD spectra, and their UV spectra (f) are identical to each other, proving that the chirality of PANI microfibers is induced by chiral dopant acid. Conditions: [G]/[P] = 35%:65%.

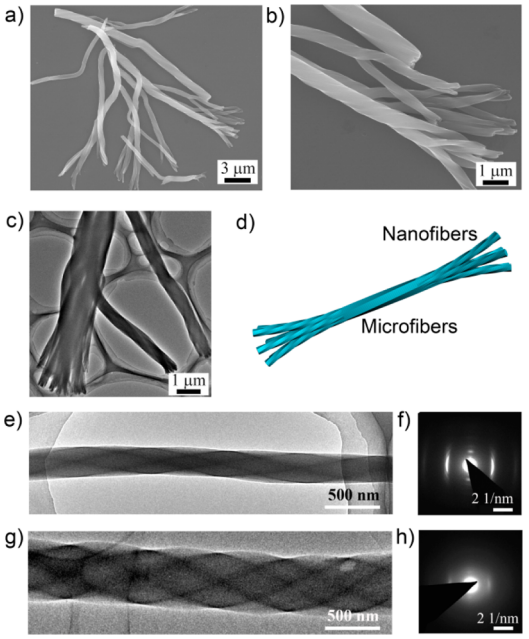

Figure 2. (a,b) SEM and TEM (c) images indicate that helical nanofibers twisted along the same direction to form superhelical microfibers. (d) Formation mechanism of PANI superhelical microfiber. (e) TEM image and (f) corresponding SAED pattern of PANI helical nanofiber. (g) TEM image and (h) SAED pattern of PANI helical microfiber showing very clear helical screws.

chiral excitonic coupling corresponding to the absorption at ~430 nm in the UV−vis−IR spectra (Figure 1f). The negative strong band at ~780 nm should be ascribed to polarons corresponding to the dominant band at ~800 nm in the UV−vis−IR spectra. In contrast, the CD spectra of right-handed helical microfibers, which were doped by R-CSA, show behavior symmetrical with those of left-handed microfibers, although their absorption spectra are almost identical.

Formation of PANI helical microfibers was performed subsequently. By carefully examining the SEM and TEM images, we found that PANI helical microfibers were formed by twisting of many helical nanofibers, as shown in Figure 2a−c. From the magnified image, helical nanofibers have the same screw direction as helical microfibers. Chiral PANI molecules self-assembled into helical nanofibers, and these nanofibers then further self-assembled into superhelical microfibers, indicating a hierarchical self-assembly behavior (the structures formed at different times are shown in Figure S3). As shown in Figure 2d, nanofibers formed first by the strong $\pi-\pi$ stacking interaction among PANI molecules, and then the single-handed helical nanofibers merged into microfibers during the self-assembly process due to the strong tendency for PANI nanostructures to aggregate.[23] PANI nanofibers with a molecular stacking similar to that of superhelical microfibers were observed in the initial stage of self-assembly (Figure S4). This process is very similar to the formation of fibrillar phases of peptides,[24,25] while much more ordered hierarchical structures formed in PANI superstructures due to a well-controlled self-assembly process.

The arrangement of PANI molecules in the nanofibers and microfibers was investigated by selected area electron diffraction (SAED) and X-ray diffraction (XRD) methods. Figure 2e−h shows the TEM images of helical nanofibers and microfibers and corresponding SAED patterns (corresponding XRD is shown in Figure S5). From the TEM images (Figure 2e,g), well-defined helical structures are clearly observed for both nanofibers and microfibers. The SAED patterns reveal that chiral PANI molecules arrange in an orderly way in helical nanofibers and microfibers. From Figure 2f, diffused reflections corresponding to d spacing of ~3.5 Å should be ascribed to the (040) reflection of $\pi-\pi$ stacking of PANI molecules, indicating they are arranged perpendicular to the long axis of the helical nanofiber.[26,27] Rather sharp reflections corresponding to d spacing of ~6.1 Å from the (100) reflection are due to the arrangement of CSA molecules between neighboring PANI chains. While the strong (001) reflection from the XRD pattern with d = 28 Å was overwhelmed by the intense transmission beam in the SAED pattern, sharp reflections were seen in the SAED pattern corresponding to $d \approx 10$ Å, possibly originating from the (003) reflection of the same diffraction family.

With ultra-ordered structures and a super-long geometry, PANI helical microfibers should be very convenient for the fabrication of devices based on single microfibers, and are expected to have excellent performance in chiral sensing, i.e., enantioselective discrimination of chiral species. Helical microfibers were first spin-coated on the silicon substrate with a ~300 nm thermally evaporated silicon dioxide top layer (Si/SiO_2). A SnO_2 nanofiber ~500 nm in diameter which served as a shadow mask was then moved to attach across to a single helical microfiber; this process was carried out on a probe station.[28] The SnO_2 nanofiber could attach onto Si/SiO_2 substrate tightly due to relatively strong van der Waals forces. A gold film 80 nm thick was then vacuum-evaporated, followed by removing the mask by the probe. The devices with two end gold electrodes are shown in Figure 3a,c.

dx.doi.org/10.1021/ja409796b | J. Am. Chem. Soc. 2014, 136, 578−581

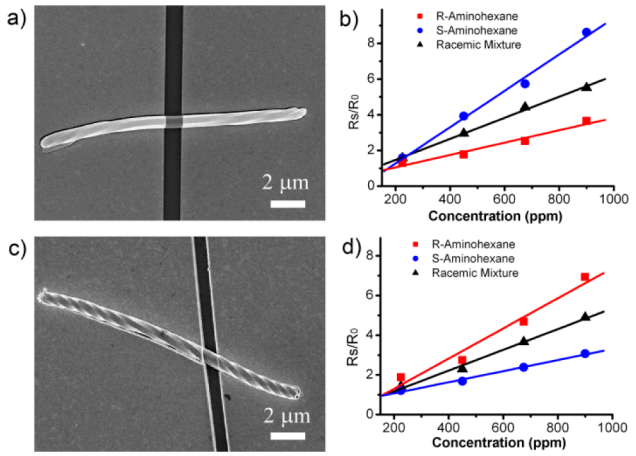

Figure 3. (a) SEM image of left-handed single-helical microfiber-based enantioselective sensor. (b) Response measurements while the device indicated in (a) was exposed to 2-aminohexane enantiomers and their racemic mixture. (c) SEM image of right-handed single-helical microfiber-based enantioselective sensor. (d) Response measurements while the device indicated in (c) was exposed to 2-aminohexane enantiomers and to their racemic mixture.

Herein, chiral aminohexane is employed as a targeted species to study the enantioselective discrimination ability of PANI helical microfibers. The device is exposed to both (*S*)-(+)-2-aminohexane and (*R*)-(−)-2-aminohexane vapor respectively by varying the concentration, and a Keithley 4200 SCS instrument is used to monitor the real-time resistance changes under an applied voltage of 0.1 V dc. The time-dependent enantioselective discrimination is denoted as relevant sensitivity (normalized resistance, R_S/R_0, where R_S and R_0 are the resistances of the device measured upon exposure to chiral aminohexane vapor and in nitrogen, respectively). The left-handed PANI microfiber-based sensor shows an obvious enantioselective discrimination to the chiral aminohexane when it is exposed to 225 ppm chiral aminohexane and the racemic mixture. The normalized resistance increases dramatically in the first 5 s, and then it takes a quite long time to reach its plateau (Figure S6). Interestingly, R_S/R_0 increased linearly with increasing concentration of chiral aminohexane. As expected, the response for the racemic mixture falls between those for the two enantiomers (Figure 3b). For right-handed PANI helical microfibers, the corresponding result showed an inverse enantioselective discrimination, which was more favorable for (*R*)-(−)-2-aminohexane (Figure 3d).

Density functional theory (DFT) calculations[29−31] were performed to investigate the chiral architecture. The planar PANI molecules prefer $\pi-\pi$ stacking along the long axis with a vertical distance about 3.5 Å, consistent with the experimental XRD data. *S*-CSA or *R*-CSA regularly lies between two adjacent PANI chains and interacts with PANI by the hydrogen bond O···H−N through the sulfonic group and NH. The distances between two neighboring CSA molecules are 6.12 and 6.55 Å, which agree well with the *d* spacing of ∼6.1 Å from the experimental XRD data. The spacing between two adjacent PANI chains is measured to be about 12.95 Å, which also agrees with the experimental data.

Furthermore, Mulliken population analysis was performed to investigate why chiral aminohexane displays enantioselective discrimination ability when it is employed as a targeted species in PANI helical microfibers. Mulliken population analysis can provide information about electron occupancy on the atoms in the system. The analysis shows that, in the PANI-S-CSA system, about 0.66 electron transfers from the PANI molecule to CSA, which is consistent with the fact that polarons are charge carriers in this system. When the chiral aminohexane is employed in the system, the aminohexane inserts between two adjacent S-CSA molecules. In the PANI-S-CSA/*S*-aminohexane system, due to their having the same chirality, *S*-aminohexane could interact with the neighboring S-CSA through the amino group and the sulfonic group, and thus more electrons transfer from the *S*-aminohexane to PANI-S-CSA system. Theoretical results reveal that employing chiral aminohexane in PANI-S-CSA system would reduce the proton on the PANI-S-CSA system. In the PANI-S-CSA/S-aminohexane system, about 0.258 electron transfers from *S*-aminohexane to PANI/S-CSA, while in the PANI-S-CSA/R-aminohexane system, about 0.205 electron transfers from *R*-aminohexane to PANI/S-CSA. This suggests that employing chiral aminohexane reduces the conducting polarons in the PANI-S-CSA system. Such a decrease in the PANI-S-CSA/*S*-aminohexane system demonstrates much more than that in the PANI-S-CSA/*R*-aminohexane system. Chiral sensing of other amines was calculated, and the analysis shows that PANI-S-CSA has the ability to enantioselectively discriminate both 2-amino-3-methylbutane and 1-aminoindane, although the sensitivity is lower than that to aminohexane (see Figure S7).

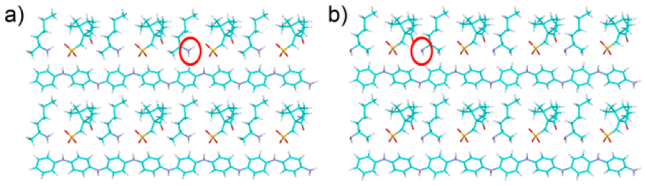

Figure 4. Theoretical analysis of enantioselective discrimination ability. (a) PANI-S-CSA inserted by (*S*)-(+)-2-aminohexane; (b) PANI-S-CSA inserted by (*R*)-(+)-2-aminohexane.

In summary, ultra-ordered, super-long, left- and right-handed PANI helical microfibers were obtained by a self-assembly process using chiral S-CSA and R-CSA as dopants, respectively. Chiral PANI molecules arranged ordered in helical microfibers with PANI molecules perpendicular to the long axis of fibers. Helical nanofibers twisted with the same screw direction to form helical microfibers, exhibiting a hierarchical self-assembly process. PANI helical microfibers showed enantioselective discrimination toward chiral aminohexane. Integrated chirality and electrical conductive properties, chiral conducting polymer structures, and their devices would be a potential platform to study the interactions between chiral supramolecular structures and chiral small molecules.

■ ASSOCIATED CONTENT

Supporting Information

Synthesis of helical PANI; preparation of helix microfibers; fabrication and characterization of chiral sensors; morphology and structure characterizations; CD spectra of PANI at different ratios of good solvent to poor solvent; XRD pattern of PANI-S-CSA; time-dependent response of the left-handed PANI microfiber exposed to 225 ppm chiral aminohexane atmosphere; computational details. This material is available free of charge via the Internet at http://pubs.acs.org.

dx.doi.org/10.1021/ja409796b | *J. Am. Chem. Soc.* 2014, 136, 578−581

AUTHOR INFORMATION

Corresponding Authors

kdeng@nanoctr.cn
jlyao@suda.edu.cn
weizx@nanoctr.cn

Author Contributions

[§]W. Zou and Y. Yan contributed equally to this work.

Notes

The authors declare no competing financial interest.

ACKNOWLEDGMENTS

This work was supported by National Natural Science Foundation of China (Grants 91027031, 21125420 and 20933008), The Ministry of Science and Technology of China (Nos. 2009CB930400, 2011CB932300, 2012CB933001), and the Chinese Academy of Sciences.

REFERENCES

(1) Toyofuku, K.; Alam, M. A.; Tsuda, A.; Fujita, N.; Sakamoto, S.; Yamaguchi, K.; Aida, T. *Angew. Chem., Int. Ed.* **2007**, *46*, 6476.
(2) Hirschberg, J.; Brunsveld, L.; Ramzi, A.; Vekemans, J.; Sijbesma, R. P.; Meijer, E. W. *Nature* **2000**, *407*, 167.
(3) Jung, J. H.; Ono, Y.; Shinkai, S. *Angew. Chem., Int. Ed.* **2000**, *39*, 1862.
(4) Wang, Y.; Xu, J.; Wang, Y.; Chen, H. *Chem. Soc. Rev.* **2013**, *42*, 2930.
(5) Hoeben, F. J. M.; Jonkheijm, P.; Meijer, E. W.; Schenning, A. *Chem. Rev.* **2005**, *105*, 1491.
(6) Kaneko, T.; Katagiri, H.; Umeda, Y.; Namikoshi, T.; Marwanta, E.; Teraguchi, M.; Aoki, T. *Polyhedron* **2009**, *28*, 1927.
(7) Avarvari, N.; Wallis, J. D. *J. Mater. Chem.* **2009**, *19*, 4061.
(8) Yashima, E.; Maeda, K.; Furusho, Y. *Acc. Chem. Res.* **2008**, *41*, 1166.
(9) Nilsson, K. P. R.; Rydberg, J.; Baltzer, L.; Inganas, O. *Proc. Natl. Acad. Sci.U.S.A.* **2004**, *101*, 11197.
(10) Palmer, L. C.; Stupp, S. I. *Acc. Chem. Res.* **2008**, *41*, 1674.
(11) Majidi, M. R.; Kanemaguire, L. A. P.; Wallace, G. G. *Polymer* **1995**, *36*, 3597.
(12) Yan, Y.; Yu, Z.; Huang, Y.; Yuan, W.; Wei, Z. *Adv. Mater.* **2007**, *19*, 3353.
(13) Li, W. G.; Wang, H. L. *J. Am. Chem. Soc.* **2004**, *126*, 2278.
(14) Yang, Y.; Zhang, Y.; Wei, Z. *Adv. Mater.* **2013**, *25*, 6039.
(15) Huang, J. X.; Egan, V. M.; Guo, H. L.; Yoon, J. Y.; Briseno, A. L.; Rauda, I. E.; Garrell, R. L.; Knobler, C. M.; Zhou, F. M.; Kaner, R. B. *Adv. Mater.* **2003**, *15*, 1158.
(16) Trojanowicz, M.; Kaniewska, M. *Electroanalysis* **2009**, *21*, 229.
(17) James, T. D.; Sandanayake, K.; Shinkai, S. *Nature* **1995**, *374*, 345.
(18) Kubo, Y.; Maeda, S.; Tokita, S.; Kubo, M. *Nature* **1996**, *382*, 522.
(19) Sheridan, E.; Breslin, C. *Electroanalysis* **2005**, *17*, 532.
(20) Zhang, F.; Ma, L.; Yang, Y.; Tang, J.; Li, X.; Qiu, W.; Tetrahedron. *Asymmetry* **2012**, *23*, 411.
(21) Feng, Z.; Li, M.; Yan, Y.; Jihai, T.; Xiao, L.; Wanglin, L. *Chirality* **2013**, *25*, 39.
(22) Torsi, L.; Farinola, G. M.; Marinelli, F.; Tanese, M. C.; Omar, O. H.; Valli, L.; Babudri, F.; Palmisano, F.; Zambonin, P. G.; Naso, F. *Nat. Mater.* **2008**, *7*, 412.
(23) Yan, Y.; Wang, R.; Qiu, X.; Wei, Z. *J. Am. Chem. Soc.* **2010**, *132*, 12006.
(24) Knowles, T. P. J.; De Simone, A.; Fitzpatrick, A. W.; Baldwin, A.; Meehan, S.; Rajah, L.; Vendruscolo, M.; Welland, M. E.; Dobson, C. M.; Terentjev, E. M. *Phys. Rev. Lett.* **2012**, *109*, 158101.
(25) Aggeli, A.; Nyrkova, I. A.; Bell, M.; Harding, R.; Mcleish, T. C. B.; Semenov, A. N.; Boden, N. *Proc. Natl. Acad. Sci. U.S.A.* **2001**, *98*, 11857.
(26) Pouget, J. P.; Hsu, C. H.; Macdiarmid, A. G.; Epstein, A. J. *Synth. Met.* **1995**, *69*, 119.
(27) Djurado, D.; Nicolau, Y. F.; Rannou, P.; Luzny, W.; Samuelsen, E. J.; Terech, P.; Bee, M.; Sauvajol, J. L. *Synth. Met.* **1999**, *101*, 764.
(28) Jiang, L.; Gao, J.; Wang, E.; Li, H.; Wang, Z.; Hu, W.; Jiang, L. *Adv. Mater.* **2008**, *20*, 2735.
(29) Delley, B. *J. Chem. Phys.* **2000**, *113*, 7756.
(30) Delley, B. *J. Chem. Phys.* **1990**, *92*, 508.
(31) Becke, A. D. *J. Chem. Phys.* **1988**, *88*, 2547.